

# Influence of laser power density on damage of comb by photodynamic therapy—simulation and validation of mathematical models

Naiyan Huang (黄乃艳)<sup>1</sup>, Zhongshun Ma (马忠顺)<sup>2</sup>, Ying Wang (王颖)<sup>1</sup>, Jing Zeng (曾晶)<sup>1</sup>,  
Haixia Qiu (邱海霞)<sup>1</sup>, Xiaoying Tang (唐晓英)<sup>2</sup>, and Ying Gu (顾瑛)<sup>1\*</sup>

<sup>1</sup>Department of Laser Medicine, Chinese PLA General Hospital, Beijing 100853, China

<sup>2</sup>School of Life Science and Technology, Beijing Institute of Technology, Beijing 100081, China

\*Corresponding author: guyinglaser@sina.com

Received September 25, 2013; accepted January 15, 2014; posted online February 28, 2014

Photodynamic therapy (PDT) has poor therapeutic outcomes for the treatment of port-wine stain (PWS) lesions with long drug-light intervals (DLIs). This letter investigates the possibility of improving the treatment efficacy through increasing the laser power density using a computer simulation and a cock comb model. The computational model includes a Monte Carlo simulation for the laser distribution and a calculation of the singlet oxygen concentrations ( $^1\text{O}_2$ ). Both simulation and experimental results show that increasing the power density from 100 to 140 mW/cm<sup>2</sup> not only improves the PDT efficacy, but also results in the unwanted skin damage.

OCIS codes: 170.5180, 170.1870.

doi: 10.3788/COL201412.031701.

Port-wine stain (PWS) lesions are vascular malformations consisting of superficial and deep dilated capillaries in the skin<sup>[1,2]</sup>, which produces a reddish to purplish skin discoloration. PWSs occur most often on the face and persist throughout life. The presence of PWSs can cause emotional and social problems for the affected person because of their cosmetic appearance.

Photodynamic therapy (PDT) is an emerging treatment field on PWS. Since Orenstein *et al.*<sup>[3]</sup> suggested that PDT might be a possible alternative to photothermal therapy for PWSs, there were thousands of PWS patients accepting PDT in Chinese clinics<sup>[4–6]</sup>. The treatment results are encouraging, especially on serious lesions with nodules and thick lesions in adult patients<sup>[7]</sup>.

The PDT reaction mechanism works by using a photosensitizer that is excited from a ground state to an excited singlet state and then undergoes an intersystem crossing to a longer-lived excited triplet state. An energy transfer to molecular oxygen and another ground triplet state can take place and create an excited singlet state oxygen molecule. Singlet oxygen ( $^1\text{O}_2$ ) is an aggressive chemical species that rapidly reacts with any nearby biomolecule. Ultimately, these destructive reactions kill cells through apoptosis or necrosis<sup>[8]</sup>.

In PDT treatment for PWS, most photosensitizers are confined within blood vessels when using shorter photosensitizer drug administrations and light illumination intervals (drug-light intervals (DLTs))<sup>[9]</sup>. A laser with a short wavelength (532 nm, 413 nm, or dual-wavelength 510 nm and 578 nm) penetrates 1 mm or less due to the strong absorption of blue and green lights by the blood in PWS lesions. Therefore, the toxic materials are generated mainly in the abnormal blood vessel chambers without damage to the surrounding tissue and the deep, normal, nutritional blood vessels. In theory, this double-selective effect of laser and photosensitizers could result in damage of PWS abnormal blood vessels while leaving the skin intact.

In the clinical context, some cases involved a large, uneven lesion, and a single light beam could not cover the entire lesion. In such cases, the lesion was divided into two or three treatment areas, and each was irradiated sequentially. However, the area treated with a longer DLI over 1 h exhibited a poor response. In our previous study, the treatment outcome of the longer DLI improved with the longer treatment time<sup>[10]</sup>. However, a computer simulation and a cock comb model were used to investigate the effect of increasing the power density in this letter.

At first, a mathematical model was established to simulate the generation of  $^1\text{O}_2$  in tissue. The tissue model in the simulation was set up according to the histology of the comb. We used the comb as the animal model for PWS because there is a large amount of dilated capillaries in the comb's shallow dermis<sup>[3]</sup>. The comb skin model contained both the epidermal (60  $\mu\text{m}$ ) and dermal

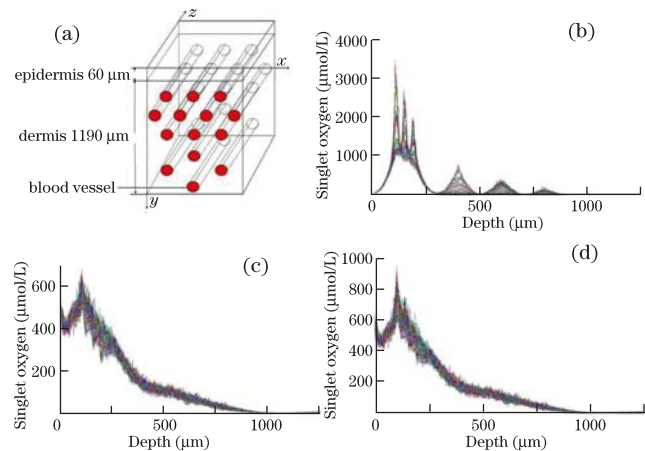


Fig. 1. (a) Schematic diagram of comb tissue; simulation results of singlet oxygen with DLIs of (b) 5 and (c) 60 min and power density of 100 mW/cm<sup>2</sup>; (d) simulation result of singlet oxygen with DLI of 60 min and power density of 140 mW/cm<sup>2</sup>.

**Table 1. Optical Parameters of Skin at 532-nm Wavelength**<sup>[14–17]</sup>

Tissues	$\mu_a$ (cm <sup>-1</sup> )	$\mu_s$ (cm <sup>-1</sup> )	$g$	$n$
Epidermis	28.6	187.5	0.78	1.37
Dermis	1.05	187.5	0.78	1.37
Blood	250	700	0.956	1.405

(60–1250  $\mu\text{m}$ ) layers with many blood vessels (Fig. 1(a)). There were six layers of blood vessels in the dermis (Fig. 1(a)). The blood vessel diameter was 20  $\mu\text{m}$  because the average diameter of the comb blood vessels was 20  $\mu\text{m}$ . The distance between the centres of two blood vessels was 40  $\mu\text{m}$  in layers 1–3 and 200  $\mu\text{m}$  in layers 4–6. The centre of each layer was at depths of 110, 150, 190, 400, 600, and 800  $\mu\text{m}$ .

The laser energy distribution in the tissue was simulated using the Monte Carlo<sup>[11,12]</sup> method with the computer codes developed by Wang *et al.*<sup>[13]</sup>. The optical properties of the comb were not reported, so we used the parameters of human skin including  $\mu_a$  (absorption coefficient, the unit is cm<sup>-1</sup>),  $\mu_s$  (scattering coefficient, the unit is cm<sup>-1</sup>),  $g$  (anisotropy factor), and  $n$  (refractive index)(Table 1). The optical properties were calculated mainly according to the method provided by Jacques<sup>[14]</sup>, which was used by many authors in computer simulation studies and in measurements of skin's optical properties<sup>[15,16]</sup>. The scattering coefficient of blood came from a previously published source<sup>[17]</sup>.

<sup>1</sup>O<sub>2</sub> is the photochemical product of three elements: a laser, a photosensitiser, and oxygen<sup>[10]</sup>. The equation is

$$\Pi_{1O_2(t)} = 2.303\varepsilon\Phi C_{m(t)} \frac{I}{S} \frac{C_{O(t)}}{C_{O(t)} + \frac{k_p}{k_t}}, \quad (1)$$

where  $\Pi_{1O_2(t)}$  is the <sup>1</sup>O<sub>2</sub> concentration,  $\varepsilon$  is mole extinction coefficient of the photosensitiser, and  $\Phi$  is the quantum yield of <sup>1</sup>O<sub>2</sub>.  $C_{O(t)}$  is the concentration of oxygen molecules, and  $C_{m(t)}$  is the concentration of the ground state photosensitiser (in this letter, the photosensitiser was haematoporphyrinmonomethyl ether, HMME). The rate constant for phosphorescence generation is  $k_p$ , and  $k_t$  is the reaction rate constant between the triplet photosensitiser and an oxygen molecule.  $S$  is the area of light irradiation, and  $I$  is the laser energy density in the simulation.

In Eq. (1),  $\Phi$ ,  $\varepsilon$ ,  $k_p$  and  $k_t$  are constants;  $\Phi = 0.6$  for HMME<sup>[18]</sup>. We measured the HMME absorption at different concentrations and calculated  $\varepsilon$  to be  $0.39 \times 10^4$  L/(mol·cm) at 532 nm. The  $k_p/k_t$  value of Photofrin (i.e., 2.5 mol/L) reported by Georgakoudi *et al.*<sup>[19]</sup> was used because the HMME was similar to Photofrin. The laser power density,  $I/S$ , was determined from the Monte Carlo simulation result. The concentrations of the photosensitiser ( $C_{m(t)}$ ) and oxygen ( $C_{O(t)}$ ) in the tissue were determined by different modelling methods as described below.

The photosensitiser concentration in the blood is different than that outside of the blood vessel. In the blood vessel, the pharmacokinetic equation was derived

as<sup>[20]</sup>

$$C = 9.9559 \exp(-0.3679t) + 0.5831 \exp(-0.1019t) + 0.2358 \exp(-0.0113t), \quad (2)$$

where  $C$  is the photosensitiser concentration in the blood vessel in  $\mu\text{g/mL}$ , and  $t$  is the time in minutes.

The photosensitiser distribution outside of the blood vessels is more complex. The photosensitiser diffuses from the blood vessels following Fick's law and is influenced by photobleaching as

$$D_m \nabla^2 C_m - \frac{\partial C_m}{\partial t} = \Gamma_{\text{PDT}}, \quad (3)$$

where  $C_m$  is the photosensitiser concentration outside of the blood vessels, and  $D_m$  is the photosensitiser diffusivity. In addition, 50  $\mu\text{m}^2/\text{s}$  was used for HMME because there was no reported value available. This value was obtained based on the  $D_m$  of glucose by comparing the average molecular weight of HMME to that of glucose.

We adopted a mathematical model of the spatial and temporal distribution of oxygen in tissue<sup>[21]</sup>, which included a metabolic oxygen consumption rate and a PDT-induced oxygen consumption rate:

$$D_s \nabla^2 C_O - \frac{\partial C_O}{\partial t} = \Gamma_1 + \Gamma_2, \quad (4)$$

where  $C_O$  is the oxygen density and  $D_s$  is the oxygen diffusivity (1500  $\mu\text{m}^2/\text{s}$ <sup>[22]</sup>).  $\Gamma_1$  is the rate of oxygen consumption by metabolism, and its value is 1.7  $\mu\text{mol}/(\text{L}\cdot\text{s})$ <sup>[23]</sup>.  $\Gamma_2$  is the rate of oxygen consumption by photodynamic reaction, which is the same as  $\Pi_{1O_2(t)}$  in Eq. (1) because each oxygen molecule is converted to <sup>1</sup>O<sub>2</sub>.

The differential equations were solved by the finite difference method, and each point in the comb tissue model was simulated using Matlab and Microsoft C++ software. Rectangular coordinates were used in the tissue model. A three-dimensional network was constructed, with a grid width of 5  $\mu\text{m}$ .

At first, we simulated the influence of DLI on PDT efficacy. When the DLI was 5 min, <sup>1</sup>O<sub>2</sub> was mainly localised in the blood vessels (Fig. 1(b)). When the DLI was 60 min, the <sup>1</sup>O<sub>2</sub> concentration in the blood vessels was almost the same as that in the surrounding tissues (Fig. 1(c)). It was clear that the amount of <sup>1</sup>O<sub>2</sub> in the blood vessels after 60 min of DLI was significantly less than that after 0 min of DLI. For example, in the first layer of blood vessels, the <sup>1</sup>O<sub>2</sub> concentration was average 2052  $\mu\text{mol/L}$  after a 5-min DLI, but only average 530  $\mu\text{mol/L}$  after a 60-min DLI. When the power density was increased to 140 mW/cm<sup>2</sup> (a relative safe dose without thermal damage), the <sup>1</sup>O<sub>2</sub> concentration increased to average 705  $\mu\text{mol/L}$  in the blood vessels, and also increased in surrounding tissue (Fig. 1(d)). These simulation results implied that the blood vessels should be destroyed by PDT with DLI of 5 min, but may be not destroyed with DLI of 60 min. When the power density was increased to 140 mW/cm<sup>2</sup>, the damage may be appeared both in the blood vessels and surrounding tissues.

For validation of these simulation results, the animal

experiment was carried out after approved by the Animal Care Committee of the Chinese PLA General Hospital. The comb of Lenhen cocks (male, 0.8–1.1 kg) were used for investigating. A treatment area ( $2 \times 2$  (cm)) in each comb was irradiated while the surrounding tissue was covered with double-layered black cloth. 5 cocks' combs (group I) were exposed to the light 5 min after the intravenous injection of the photosensitizer (DLI=5 min), and 5 cocks combs (group II) were treated 1 h later (DLI=60 min). Both group I and group II were irradiated with a power density of  $100 \text{ mW/cm}^2$  for 20 min. In group III ( $n = 5$ ), the combs were irradiated with a power density of  $140 \text{ mW/cm}^2$  and DLI of 60 min. the photosensitizer HMME with  $10 \text{ mg/kg}$  was produced by Shanghai Zhangjiang Corporation, China. The 532-nm KTP laser which supplied by Tianjin Medical University was a quasi-continuous model with a pulse repetition frequency of 10 kHz and a pulse width of 50 ns. The light was delivered through an optical fibre with a flat cut tip to irradiate comb surface. All irradiation times were 20 min.

Cocks were kept in dimmed lighting after PDT. The gross changes of the comb were visually examined daily and were recorded by a digital camera. When the DLI was 5 min, the colour of all 5 combs in group I was initially pink but changed to purple (immediately after PDT) (Fig. 2(a)), dark purple (24 h later) (Fig. 2(b)), and purple and white (72 h later) (Fig. 2(c)). When the DLI was 60 min, the colour of all 5 combs in group II was light red when the irradiation stopped (Fig. 2(e)), and it returned to its original colour 24 h later (Fig. 2(f)). With a 60-min DLI and a power density of  $140 \text{ mW/cm}^2$ , the comb colour in group III changed to light purple 24 h later, but blisters were observed on the combs of 4 out of 5 cocks 24 h later (Figs. 2(i) and (j)). The blisters broke 48 h later, which resulted in skin necrosis (Fig. 2(k)). The last comb had a small blister that healed 3 days later.

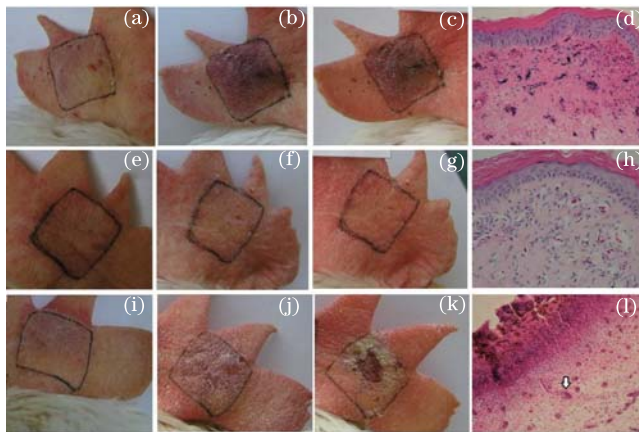


Fig. 2. (Color online) Macroscopic changes of comb in group I at (a) 0, (b) 24, and (c) 72 h after PDT; (d) pathological examination of the comb shows that thrombi are formed in the capillary vessels. Macroscopic changes of comb in group II at (e) 0, (f) 24, and (g) 72 h after PDT; (h) normal structure appeared in comb, macroscopic change of comb in group III at (i) 0, (j) 24, and (k) 72 h after PDT; (l) pathological examination shows that necrosis appear from epidermis to dermis, and thrombi are appeared in blood vessels under necrosis tissue. Arrow indexes thrombus in dermis. (H. E.  $\times 200$ ).

The comb biopsy was procured 72 h after PDT for standard H.E. staining, and histopathological examinations were conducted by one pathologist. A pathological examination showed that thrombi formed in the capillary vessels of the papillary dermal layer and the shallow reticular layer when the DLI was 5 min (in all 5 combs) and that the epidermal and dermal structures were normal (without necrosis) (Fig. 2(d)). When the DLI was 60 min, the epidermis, dermis and vessels were normal (Fig. 2(h)) (in all 5 combs). For group III, necrosis appeared from the epidermis to the dermis (Fig. 2(l)), and under this necrotic tissue, thrombi formed in deep sites.

The mathematical models are useful tools in the research of PDT<sup>[24,25]</sup>. The mathematical models could be different according to the research issues<sup>[26]</sup>. In this letter we focused on the generation of  $^1\text{O}_2$  in the vessels because  $^1\text{O}_2$  was the most important substance generated in PDT<sup>[27]</sup>, and it caused tissue damage and therapeutic efficiency in clinic. So a relatively simplified mathematical model was established to simulate the generation of  $^1\text{O}_2$  in comb model during PDT. The simulation results of this mathematical model were helpful in the choice of optimal laser wavelength in clinic<sup>[28,29]</sup>. In this letter, the same mathematic model simulated the influence of power density on the generation of  $^1\text{O}_2$ , and the results were validated by the animal experiment. The simulation result showed that a higher  $^1\text{O}_2$  concentration was generated in the blood vessels when the DLI was 5 min, and the comb colours in group I changed to white and thrombi formed in the blood vessels, which meant the damage only in blood vessels. When the simulation result showed less  $^1\text{O}_2$  in the blood vessels with the DLI of 60 min, both the comb colour and the pathological examination seemed normal in group II. In group III, both the blood vessels damage and the skin necrosis in the combs were consistent with more  $^1\text{O}_2$  generation in both blood vessels and surrounding tissues with the DLI of 60 min and a power density of  $140 \text{ mW/cm}^2$ . These results demonstrated that increasing the power density in PDT with longer DLI would destroy both the blood vessels and the surrounding tissues. It was not safe because the damage of surrounding tissues could result scar.

Although the simulation results showed the same trend of tissue response in animal experiment, we were still hard to identify the damage threshold of  $^1\text{O}_2$  on tissue. One reason maybe that the mathematical model was simplified and the optical parameters were not tested using comb tissue. More research work need to be done to increasing the accuracy of this model.

In conclusion, according to mathematic simulation and animal experimental results, increasing power density is not an optimal protocol to improve PDT efficient in the condition of longer DLI, because the  $^1\text{O}_2$  generated in surrounding tissues increases with increasing power density, and results in the unwanted damage of normal tissue. We should look for other safe way to achieve better treatment result.

This work was supported by the Key Program of National Natural Science Foundation of China (No. 61036014) and the National Natural Science Foundation of China (No. 31170963).

## References

1. L. Winer and B. Hills, *Califor Med.* **77**, 242 (1952).
2. C. J. Chang, J. S. Yu, and J. S. Nelson, *J. Formos Med. Assoc.* **107**, 559 (2008).
3. A. Orenstein, J. S. Nelson, L. H. Liaw, R. Kaplan, S. Kimel, and M. W. Berns, *Lasers Surg. Med.* **10**, 334 (1990).
4. Y. Gu, N. Huang, J. Liang, Y. M. Pan, and F. G. Liu, *Ann. Dermatol. Venereol.* **134**, 241 (2007).
5. Z. Huang, *Photodiagn. Photodyn. Therapy* **3**, 71 (2006).
6. Y. Zhao, Z. Zhou, G. Zhou, P. Tu, Q. Zheng, J. Tao, Y. Gu, and X. Zhu, *Photoderm, Photoimmun Photomed* **27**, 17 (2011).
7. K. Yuan, Q. Li, W. L. Yu, D. Zeng, C. Zhang, and Z. Huang, *Photodiagn. Photodyn. Therapy* **5**, 50 (2008).
8. E. Buytaert, M. Dewaele, and P. Agostinis, *Biochim. Biophys. Acta Rev. Cancer* **1776**, 86 (2007).
9. B. Chen, B. W. Pogue, P. J. Hoopes, and T. Hasan, *Crit. Rev. Eukar. Gene Express* **16**, 279 (2006).
10. N. Huang, G. Cheng, X. Li, Y. Gu, F. Liu, Q. Zhong, Y. Wang, J. Zen, H. Qiu, and H. Chen, *Photodiagn. Photodyn. Therapy* **5**, 120 (2008).
11. R. Valentine, K. Wood, C. Brown, S. Ibbotson, and H. Moseley, *Phys. Med. Biol.* **57**, 6327 (2012).
12. C. Zhu and Q. Liu, *J. Biomed. Opt.* **18**, 050902 (2013).
13. L. Wang, S. L. Jacques, and L. Zheng, *Comput. Methods Programs Biomed.* **47**, 131 (1995).
14. S. L. Jacques, "Skin Optics," Oregon Medical Laser Center News, <http://omlc.ogi.edu/news/jan98/skinoptics.html> (1998).
15. S. H. Tseng, P. Bargo, A. Durkin, and N. Kollias, *Opt. Express* **17**, 14599 (2009).
16. R. Chen, Z. Huang, H. Lui, I. Hamzavi, D. I. McLean, S. Xie, and H. Zeng, *J. Photochem. Photobiol. B* **86**, 219 (2007).
17. M. Friebel, A. Roggan, G. Müller, and M. Meinke, *J. Biomed. Opt.* **11**, 034021 (2006).
18. J. Chen, Y. Lu, S. Chen, and H. Cai, *Photogr. Sci. Photochem.* **9**, 156 (1991).
19. I. Georgakoudi, M. G. Nichols, and T. H. Foster, *Photochem. Photobiol.* **65**, 135 (1997).
20. N. Huang, Y. Gu, F. Liu, G. Cheng, Q. Zhong, Y. Wang, H. Qiu, L. Liu, and J. Zeng, in *Proceedings of IEEE Conference on International Conference on Complex Medical Engineering* 1172 (2007).
21. K. K. H. Wang, S. Mitra, and T. H. Foster, *Med. Phys.* **34**, 282 (2007).
22. M. Nichols and T. Foster, *Phys. Med. Biol.* **39**, 2161 (1994).
23. T. H. Foster, R. S. Murrant, R. G. Bryant, R. S. Knox, S. L. Gibson, and R. Hilf, *Radiat. Res.* **126**, 296 (1991).
24. B. Liu, T. J. Farrell, and M. S. Patterson, *Phys. Med. Biol.* **55**, 5913 (2010).
25. B. Liu, T. J. Farrell, and M. S. Patterson, *J. Biomed. Opt.* **17**, 0880011 (2012).
26. W. Cai and L. Ma, *Chin. Opt. Lett.* **10**, 012901 (2012).
27. B. Li, H. Lin, D. Chen, M. Wang, and S. Xie, *Chin. Opt. Lett.* **8**, 86 (2010).
28. N. Huang, G. Cheng, Y. Wang, J. Zeng, H. Qiu, and Y. Gu, *Lasers Med. Sci.* **26**, 665 (2011).
29. Y. Wang, Y. Gu, Z. Zuo, and N. Huang, *J. Biomed. Opt.* **16**, 098001 (2011).